Copyright © 1977 American Telephone and Telegraph Company
THE BELL SYSTEM TECHNICAL JOURNAL
Vol. 56, No. 3, March 1977
Printed in U.S.A.

Photon Probe—An Optical-Fiber Time-Domain Reflectometer

By S. D. PERSONICK

(Manuscript received May 14, 1976)

This paper describes an optical time-domain reflectometer that incorporates a gated photomultiplier receiver. The instrument can detect extremely weak reflections from fiber breaks (more than 65 dB below the 4-percent reflection of a perfect break) with 0.5-m distance resolution. In addition, backward Rayleigh scattering, which occurs roughly uniformly along a fiber, can be used to estimate the attenuation vs position within a fiber. Therefore, regions of high attenuation can be located nondestructively from one end of the fiber.

I. INTRODUCTION

Time-domain reflectometers for locating breaks in optical fibers have been implemented by a number of researchers[1,2]. Typically, these instruments have incorporated GaAs injection lasers to produce pulses of light having a high peak power and a narrow width and have incorporated avalanche photodiode (APD) receivers. The present instrument incorporates a gated photomultiplier receiver, specifically designed for this application. The photomultiplier allows increased sensitivity compared to the APD receivers and its gating action allows the user to "look behind" large reflections that otherwise would cause undesirable saturation of the receiver.

The instrument is capable of detecting echos from breaks or imperfections that are 65 dB below the 4-percent echo from a perfect break. The distance resolution is 0.5 m.* By using a transmitted pulse that is wider or narrower (the present pulse is 5 ns in duration), a trade-off between sensitivity and resolution can be made.

In addition, the backward Rayleigh scattering, which occurs roughly uniformly along the fiber, can be used to estimate the loss as a function

* The delay per unit length of light in glass is 5 ns/m. The 5-ns *full-width* transmitted pulse gives a delay resolution of 0.5 m without special signal processing.

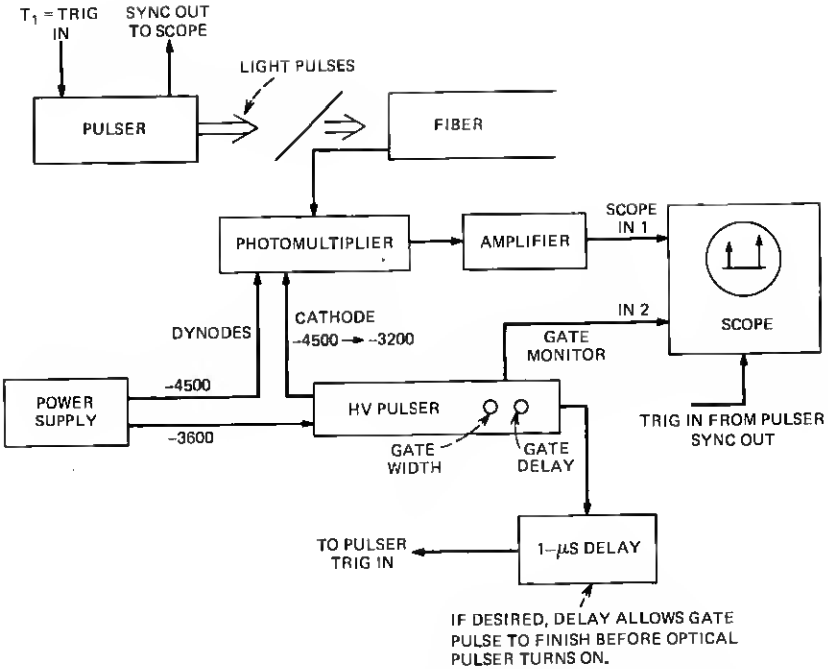

Fig. 1—Optical time-domain reflectometer.

of position along the fiber (see Section IV for a clarification of Rayleigh scattering). Thus, the loss uniformity can be estimated and regions of high loss can be identified nondestructively from one end of the fiber.

II. SYSTEM DESCRIPTION

The basic system is shown in Fig. 1. The light source is a large optical cavity, 8250-Å injection laser driven by an avalanche transistor. Drivers of this type have been described in the literature.[3] Pulse widths below 150 ps can be obtained, but the present system operates with a 5-ns transmitted pulse width. This was chosen as a compromise between resolution in the arrival time of the echo returns and pulse energy. The pulse-repetition rate is 5 KPPS. The laser output is collimated by a lens and passes through a beam splitter that serves as a directional coupler. The beam is then focused onto the fiber to be measured. (If only one end of the test fiber is available, the system is aligned with a short "pigtail" fiber of the same type as the test fiber; the test fiber is then spliced on to the pigtail.)

Echoes from the fiber (including echoes from the front face or from splices used to attach the test fiber to the pigtail) are directed by the beam splitter to the cathode of a gated electrostatic photomultiplier. The

photomultiplier cathode has a quantum efficiency of about 8 percent at this wavelength. It is mounted in a thermoelectrically cooled housing to minimize dark current and maximize cathode life. The multiplication factor of the tube is about 2×10^5. It is quantum noise limited when interfaced with commercial 50-ohm amplifiers. The tube has two features incorporated specifically for this application. The dynode chain draws current from a high-impedance divider network that limits the dynode current under high-light-level conditions. This minimizes the chances of damage due to light overload or abuse. In addition, the tube can be gated off by raising the cathode potential approximately 1000 V above its nominal −4500 V potential. This gating feature eliminates the saturation, caused by strong nearby echoes, that is present when using APD or PIN diode receivers.

The high-voltage gate pulses are obtained from a gate generator rated at 55-ns rise and fall times with a 30-pF, purely capacitive load. This is consistent with the performance measured with the present instrument. In this system, the photomultiplier turns on when the gate pulse turns off. The gate-pulse width is adjustable from 750 ns to 100 ms. Using the adjustable delays available on the generator, the gate pulse can be positioned to turn the tube on immediately after any undesired echo has arrived.

III. PERFORMANCE

Measurements of reflections (echo scans) using the optical TDR ("photon probe") are shown in Figs. 2 through 11.

Figure 2 shows the echo scan for a short fiber 70 m long. The fiber round-trip loss is negligible. The fiber numerical aperture (NA) is about 0.2. In the figure, we can see the saturated front-face reflection (no gating is applied) and the saturated back-face reflection, both of which appear as large exponentially decaying pulses. The saturation effects shown can be reduced somewhat by using a different amplifier following the photomultiplier. However, experiments reveal that without gating there is a long-term reduction (approximately 3 dB) of the photomultiplier gain which persists for tens of microseconds after overload of the tube with a large echo. When gating is used, this long-term reduction of the gain is eliminated. (See also the discussion of Figs. 6 through 8.) This long-term gain reduction is associated with the time constants of the photomultiplier burnout-prevention circuit. A double-round-trip reflection can also be seen at about 28 dB down (4 percent by 4 percent) from the back-face echo.

Figure 3 shows the echo scan for the 70-m fiber with gating of the front-face echo. The gating voltage was adjusted to leave a small remnant of the front-face echo, although complete gating is possible. The delay between the front-face echo remnant and the onset of Rayleigh-scat-

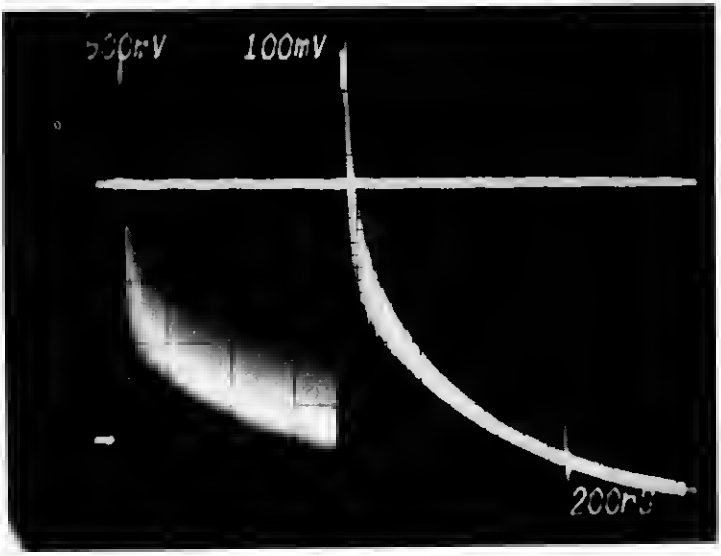

Fig. 2—Echo scan for a 70-m optical fiber.

tering reflections (the noise-like part of the trace) represents the resolution of the gating mechanism. The upper trace represents the position of the falling edge of the gating pulse. Fluctuations on the baseline of the Rayleigh scattering are due to pick up from the high-voltage gate gen-

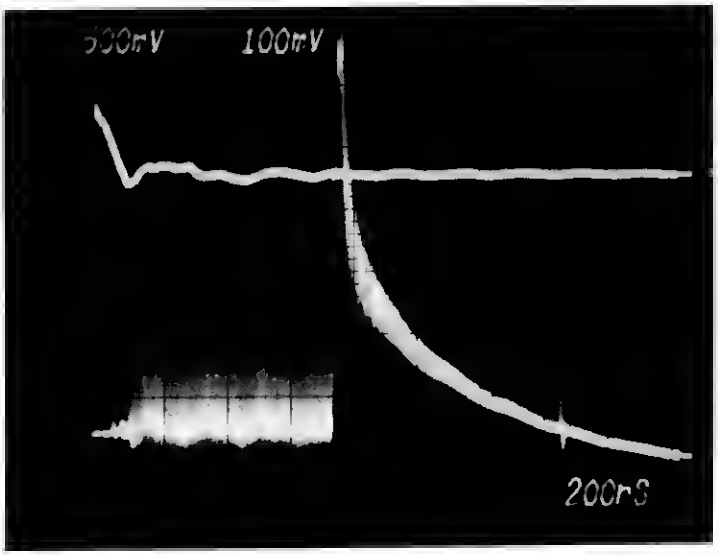

Fig. 3—Echo scan for a 70-m optical fiber with gating of front-face echo.

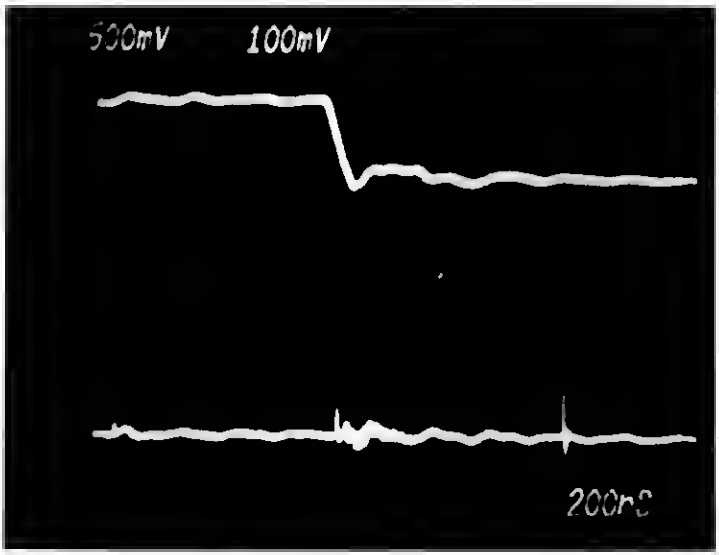

Fig. 4—Echo scan for a 70-m optical fiber with front- and back-face echoes gated out.

erator. Since the round-trip loss in this short fiber is much less than 1 dB, there is no decay in the Rayleigh scattering trace as a function of delay (distance along the fiber).

Figure 4 shows the echo scan for the 70-m fiber as above with front- and back-face echoes gated out. Note that there is no noise-like trace following the back-face echo. This is one confirmation that the noise-like trace is Rayleigh scattering and not dark current or a residue of the front-face echo.

Figure 5 shows the echo scan for the 70-m fiber with no gating and with 65 dB of optical pad between the beam splitter and the photomultiplier. The front- and back-face reflections are weak but visible.

Figure 6 shows the echo scan for a 600-m low-loss fiber with a 0.2 NA. No gating is applied. The amplifier following the photomultiplier in this measurement recovers quickly from overload, so the saturation effects due to the overload of the front-face echo are not as obvious. The decay in the Rayleigh scattering part of the trace is due to fiber attenuation vs length.

Figure 7 shows the same trace as Fig. 6 after boxcar averaging with a 0.5-s integration time and a 50-s total sweep time. No gating is applied.

Figure 8 shows the same trace as Fig. 7, but with gating of the front-face echo. The fine structure on this trace is system noise (laser pulse-amplitude fluctuations), and is not indicative of fiber details. However, the rate of decay of the roll off of the Rayleigh scattering and its shape

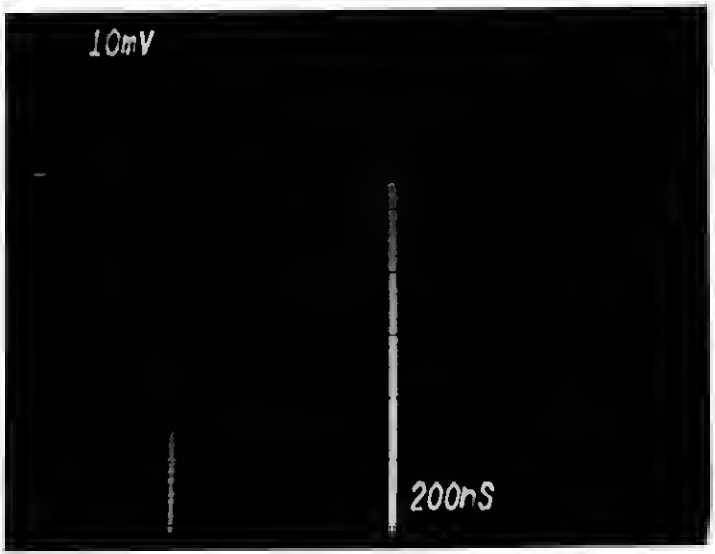

Fig. 5—Echo scan for a 70-m optical fiber with no gating and 65-dB optical pad.

are measures of the fiber loss and uniformity. With improvements in the laser pulser and the signal-processing technique, it is anticipated that fine structure in the loss vs length dependence will be obtainable.

Figure 9 shows the first attempt to use this instrument to analyze a

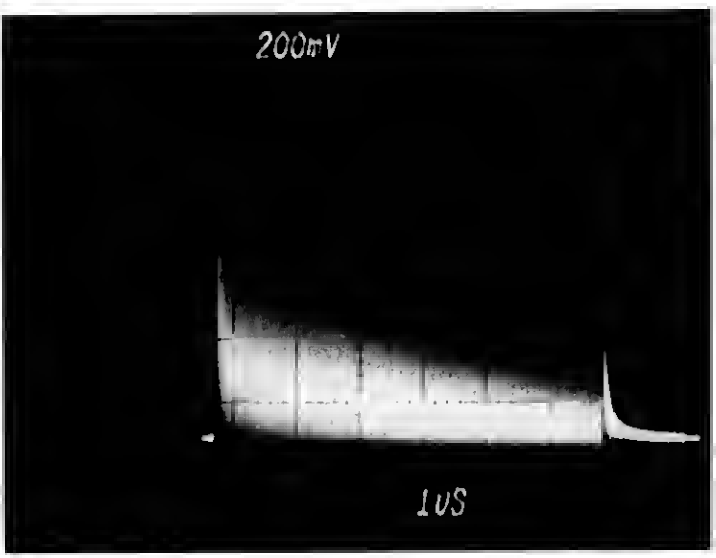

Fig. 6—Echo scan for a 600-m optical fiber before boxcar averaging.

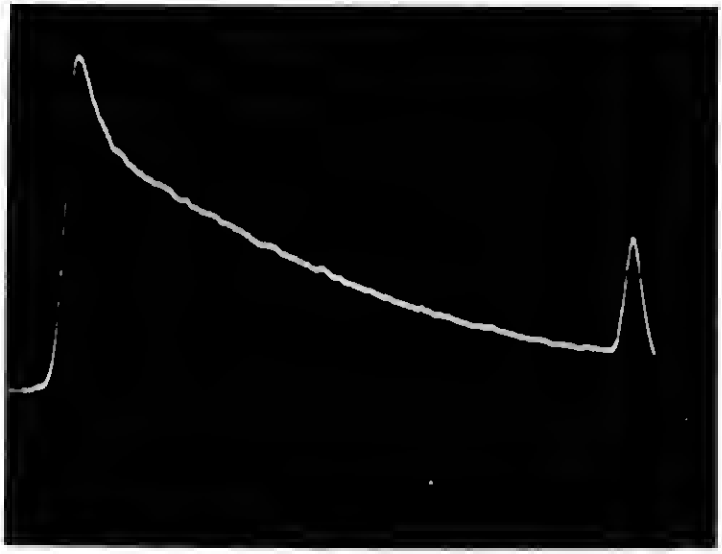

Fig. 7—Echo scan for a 600-m optical fiber after boxcar averaging.

fiber with unexplained high loss. An echo scan was obtainable from only one end and is shown before averaging. The total loss was stated as 20.8 dB, but no end-to-end transmission through the fiber was obtainable.

Figure 10 is the boxcar integrated version of Fig. 9 including front-face

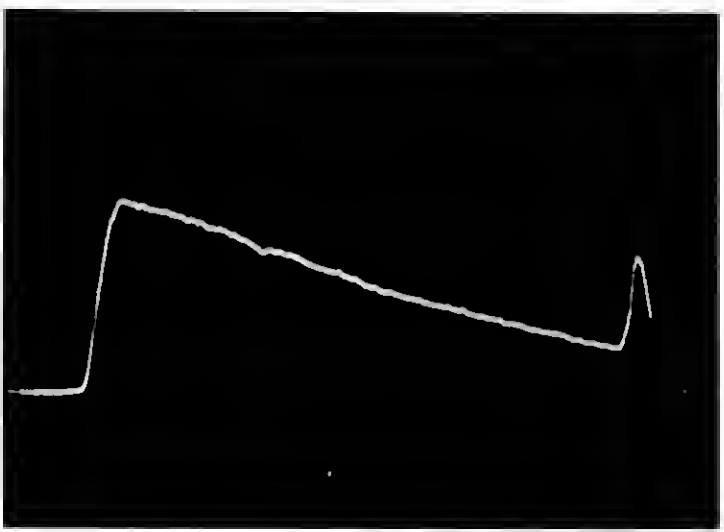

Fig. 8—Echo scan for a 600-m fiber after boxcar averaging and with gating of front-face echo.

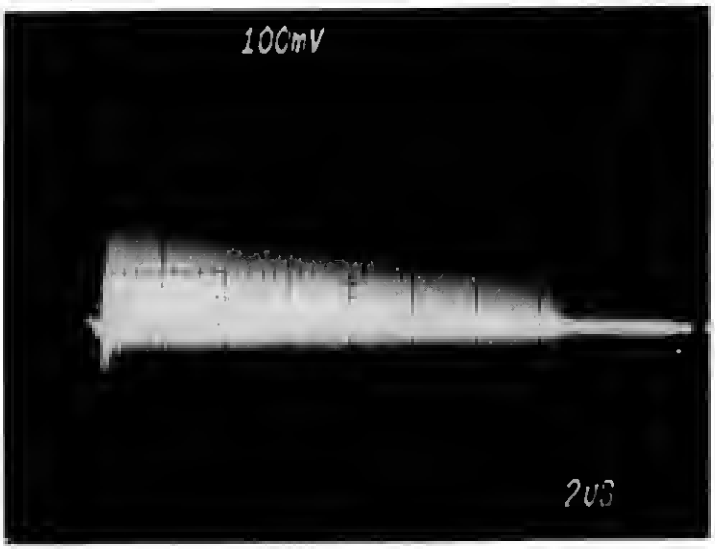

Fig. 9—First analysis of optical fiber with unexplained high loss.

echo gating. The integrating time is 0.5 s and the total sweep time is about 210 s. We see that the fiber has a rapid decay in Rayleigh scattering beginning at about 14.6-μs delay (obtained from the time scale on Fig. 9). Also, no back-face reflection is seen (compare Fig. 10 with Fig. 8). The

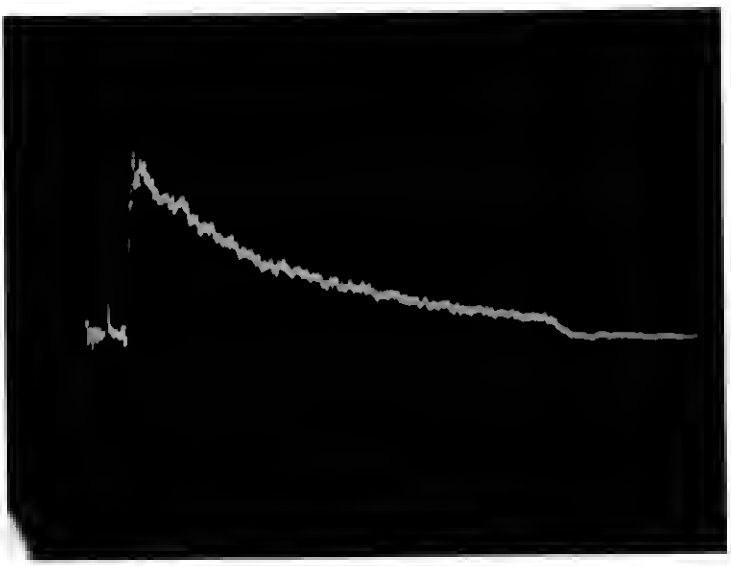

Fig. 10—Boxcar averaged version of echo scan of Fig. 9.

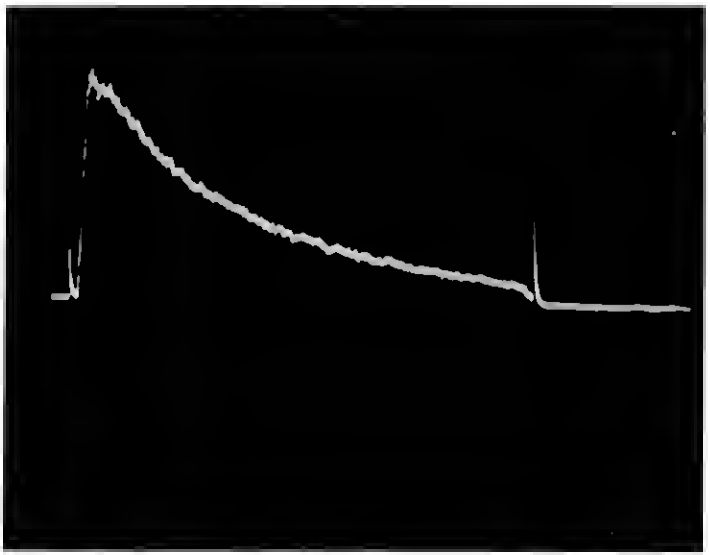

Fig. 11—Boxcar averaged scan of high-loss optical fiber after removal of lossy section.

fiber was stated as being 1500 m in length. The round-trip delay is about 10 ns/m. From this we deduce that most of the high fiber loss is concentrated in the last 50 m of one end of this fiber.

Figure 11 is the boxcar averaged trace of the high-loss fiber after removal of 120 m from the lossy end. A back-face echo is now visible. The fiber was apparently about 1570 m long. Note that not all of the high-loss region has been removed.

Figure 12 (upper trace) is a repeat of Fig. 11 using a logarithmic amplifier. The lower trace is a repeat of the upper trace with 3 dB of optical pad placed in front of the photomultiplier. This calibrates the loss-vs-length measurement (the spacing between the curves is 1.5 dB of *one-way* loss) and verified the accuracy of the logarithmic converter. The uniform loss-vs-length of the fiber can also be seen.

IV. THEORETICAL RESULTS

All of the fibers measured above were coated and wound loosely on a foam-plastic drum. No attempt was made to strip cladding modes, but this was done in tbe first few meters by the coating. A rough calculation of the expected level of Rayleigh backscattering was made as follows.*

* Rayleigh scattering is caused by variations in the density or composition of the fiber material on a scale that is small compared to the light wavelength. In state-of-the-art low-loss fibers, this is the dominant loss mechanism at 0.8-μm wavelength.

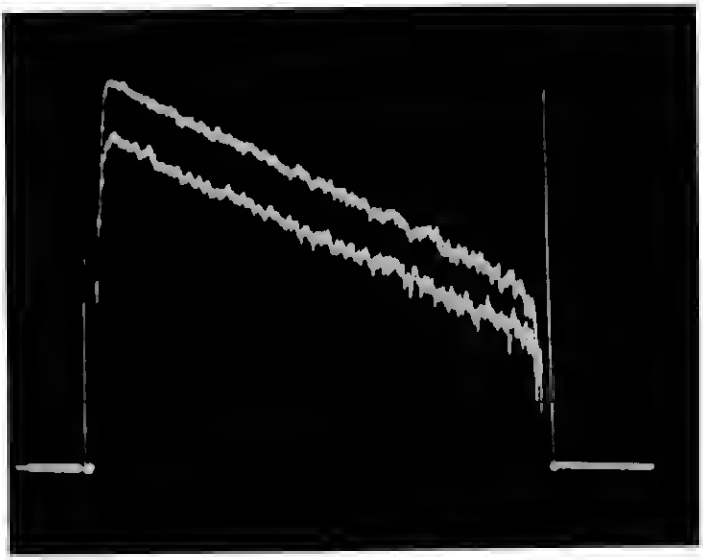

Fig. 12—Upper trace is same as Fig. 11 on logarithmic scale. Lower trace is same as upper trace with 3-dB added optical loss.

If an impulse of light of energy 1 joule is launched into the fiber, the pulse energy at a distance l (meters) along the fiber will be

$$E(l) = \exp[-\alpha(l)] \quad \text{(joules)}, \tag{1}$$

where $\alpha(l)$ is the cumulative attenuation up to distance l in nepers. In the distance interval $l + dl$, the Rayleigh-scattered energy from the fiber will be

$$dE_s(l) = \alpha_s \exp[-\alpha(l)]dl \quad \text{(joules)}, \tag{2}$$

where α_s is the Rayleigh-scattering loss in nepers per meter (assumed constant).† Of this scattered light, a fraction S will be recaptured traveling back down the fiber toward the transmitter.* At a time $t = 2l/c$, where c is the speed of light (m/s), this scattered return will arrive at the transmitter end with energy

$$\partial E_{s.echo} = S\alpha_s \exp[-2\alpha(l)]dl \quad \text{(joules)} \tag{3}$$

and will produce a response that has duration $2dl/c$. Thus, the amplitude (power) of the scattered echo at time t is

$$p(t) = \frac{cS\alpha_s}{2} \exp\left[-2\alpha\left(\frac{ct}{2}\right)\right] \quad \text{(watts)}. \tag{4}$$

* It is possible that the Rayleigh scattering from the fiber is not independent of position, and thus α_s should be replaced by $\alpha_s(l)$ in such cases. Also, there is a possibility of other (nonisotropic) types of scattering (e.g., Mie scattering from air bubbles) which do not have the same fractions, S, of recaptured light as Rayleigh scattering. Thus, in some cases S may be a function of l as well.

Thus, (4) represents the backscatter impulse response of the fiber. The fraction of scattered light recaptured is given by (assuming Rayleigh scattering is approximately isotropic)

$$S \cong \frac{\pi(\mathrm{NA})^2}{4\pi n^2} = \frac{(\mathrm{NA})^2}{4n^2}, \tag{5}$$

where NA = fiber numerical aperture (approximately 0.2 for the fibers used), n is the fiber index of refraction (approximately 1.5), and NA/n represents the half angle of the cone of captured rays. Thus, for the fibers used, S is approximately 0.005. For the fibers used in these experiments, α_s is about 4 dB/km or 0.0009 nepers/m at 0.82-μm wavelength. Thus, the backscatter impulse response is approximately

$$p(t) = 2.3 \times 10^{-6} c \exp\left[-2\alpha\left(\frac{ct}{2}\right)\right].$$

If the transmitted pulse in an actual measurement has peak power P_0 and width W, the backscattered power vs time is*

$$P_{\text{Total backscatter}} = P_0 S \alpha_s W c \exp\left[-2\alpha\left(\frac{ct}{2}\right)\right]$$

$$\cong P_0 \times 2.3 \times 10^{-6} \exp\left[-2\alpha\left(\frac{ct}{2}\right)\right]$$

$$\text{for} \quad c = 2 \times 10^8, \quad W = 5 \times 10^{-9} \text{ seconds.}$$

Thus, the backscatter power for a 5-ns transmitted pulse is about 43 dB below the 4-percent reflection of a perfect break.

The backscatter can be increased by using a wider transmitted pulse with a corresponding loss of resolution. The above result is consistent with Fig. 3 where the backscattering can be compared to the double-round-trip reflection, which is roughly 28-dB down from a perfect break reflection.

V. CONCLUSIONS

Using the above apparatus, we can detect extremely weak reflections from fiber breaks and imperfections. In addition, backward Rayleigh scattering can be used to estimate the loss as a function of position within the fiber nondestructively from one end.

The precise measurement of loss is a complicated process which requires great care to specify and control launching conditions and to obtain repeatability. The present apparatus is not intended as a sub-

* This equation assumes that $\exp[-2\alpha(ct/2)]$ is approximately constant for intervals of time t of duration W (pulse width). Otherwise one must use the average value of $\exp[-2\alpha(ct/2)]$ over the interval $(t, t + W)$.

stitute method of precise loss measurements, although refined versions of this apparatus could possibly serve that purpose. However, using this instrument, loss uniformity can be determined and concentrated loss sections in a fiber or cable can be located. In addition, fiber breaks can be located.

VI. ACKNDWLEDGMENT

The author wishes to thank R. Klein and R. Enck of Varian Corp. for their help in providing the gated photomultiplier and advice in its use. The author also wishes to thank J. S. Cook for encouragement in these experiments.

REFERENCES

1. C. Y. Boisrobert, "Some New Engineering Considerations For Fiber Optic Transmission Systems," Proceedings of the Topical Meeting on Optical Fiber Transmission, January 7–9, 1975, Williamsburg, Virginia. Sponsored by Laser and Electro-Optics Technical Group, Optical Society of America.
2. Y. Ueno and M. Shimizo, "An Optical Fiber Fault Locating Method," IEEE J. Quantum Electron., *QE-11*, No. 9, p. 77D.
3. J. R. Andrews, "Inexpensive Laser Diode Pulse Generator for Optical Waveguide Studies," Rev. Sci. Instrum., *45*, No. 1 (January 1974), pp. 22–24.